A magnetoelastic study of Cr-Fe alloys

1992 J. Phys.: Condens. Matter 4 3835

(http://iopscience.iop.org/0953-8984/4/14/014)

J. Phys.: Condens. Matter 4 (1992) 3835–3846. Printed in the UK

A magnetoelastic study of Cr–Fe alloys

H L Alberts and J A J Lourens

Department of Physics, Rand Afrikaans University, PO Box 524, Johannesburg 2000, South Africa

Received 17 December 1991, in final form 3 February 1992

Abstract. Measurements are reported of the temperature variation of the sound velocity and thermal expansion of 18 polycrystalline Cr–Fe alloys in the concentration range from 0.5 to 30 at.% Fe which covers the antiferromagnetic, spin-glass, re-entrant spin-glass, and ferromagnetic phases. In the antiferromagnetic phase, well defined anomalies in both the longitudinal velocity of sound and the thermal expansion coefficient were observed at the transition temperatures. The magnetic contributions to the volume strain ($\Delta\omega$) and bulk modulus (ΔB) have been found to fit the equations $\Delta\omega = \sum_{n=0}^{2} A_n T^{2n}$ and $\Delta B = \sum_{n=0}^{2} B_n T^{2n}$ rather well up to temperatures close to the Néel temperature. In the spin-glass phase, anomalies in the velocity of sound were observed between 4 and 150 K. These anomalies could not be attributed solely to spin-glass transitions as antiferromagnetism may still exist in these Cr–Fe alloys. In the ferromagnetic region no anomalies in either the velocity of sound or thermal expansion were observed at the Curie temperatures.

1. Introduction

The magnetoelastic properties of alloys showing spin-glass (SG) and re-entrant spin-glass (RSG) phases are of current interest [1, 2]. It has been found [3–6] that the ultrasonic longitudinal sound velocity (v_L) and therefore also the elastic constant (c_L) associated with this mode, have a broad minimum below the spin-glass transition temperature T_g. This softening in the longitudinal mode below T_g was observed in Cu–Mn [3, 5] and Au–Cr [7] spin-glasses but not in Fe–Al [1] spin-glasses. On the theoretical side, Hertz *et al* [8] used a time-dependent Landau–Ginsburg model to show that the speed of sound should decrease linearly with $(T - T_g)$ when T_g is approached from high temperatures. The data of Huang [5] however follow a more complicated function. Evidently, further investigation of spin-glasses is needed, particularly of alloy systems in which SG and RSG phases can be induced by variations of composition.

In this paper we report measurements of elastic constants (velocity of sound) and the thermal expansion of Cr–Fe alloys in the antiferromagnetic, SG, RSG and ferromagnetic phases. Spin density wave (SDW) antiferromagnetic ordering is maintained [9] in Cr–Fe alloys up to 16 at.% Fe while ferromagnetism is found above 19 at.% Fe. SG behaviour occurs for concentrations between 16 and 19 at.% Fe. RSG behaviour is observed for $10 < c < 16$ at.% Fe and for $19 < c < 28$ at.% Fe [10]. Previous [11] magnetoelastic measurements on Cr–Fe alloys containing 1.95, 2.6, 3.8, 6.65, 24.9, and 38.7 at.% Fe have been extended to include the concentration range for SG and RSG formation as well as the range below the triple point at ~2 at.% Fe [12] where the

0953-8984/92/143835+12$04.50

incommensurate (I) SDW, commensurate (C) SDW and paramagnetic phases coexist. The study includes all magnetic phases up to 30 at.% Fe in detail. Special attention is given to the concentration range around the triple point and in the SG region.

2. Experimental procedure

Cr–Fe alloys containing 0.5, 1.0, 1.5, 1.8, 2.0, 2.5, 4, 5, 8, 10, 12, 15, 16, 17, 18, 20, 25 and 30 at.% Fe were prepared by arc melting in a purified argon atmosphere from 99.99% pure starting material. One sample of each composition was prepared. They were homogenized at 1000 °C for 72 hours; those for $c \leqslant 10$ at.% Fe were furnace cooled and the others were quenched in water. X-ray powder methods revealed that the alloys were single phase. The concentrations given above are the nominal concentrations. Electron microprobe analyses on six representative samples indicated that the actual concentration does not differ by more than 5% of the nominal value and that the alloys are homogeneous to within less than 5% of the quoted concentrations. Cylinders, with lengths between 6 mm and 7 mm and diameters of 10 mm, were spark cut from the ingots and each was prepared for velocity of sound (10 MHz) and thermal expansion measurements by spark planing. The experimental techniques for the measurements are described elsewhere [13].

The thermal expansion measurements were carried out relative to Cr + 5 at.% V which remains paramagnetic at all temperatures and serves to simulate the non-magnetic component of the thermal expansion of Cr and its alloys [13]. To obtain the magnetic contribution to $c_L = \rho v_L^2$, where ρ is the density of the sample, we used [13] c_L of Cr + 5 at.% V to represent the non-magnetic component of the Cr–Fe alloys:

$$\Delta c_L(\text{Cr–Fe}) = c_L(\text{Cr + 5 at.\% V}) - c_L(\text{Cr–Fe}).$$

Since the bulk modulus $B = c_L - \frac{4}{3}c_T$, where $c_T = \rho v_T^2$ and v_T is the shear velocity, and since we found no (or negligibly small) magnetic contributions to c_T, we approximate ΔB by Δc_L. The error in the absolute values of the sound velocity varies between 0.5 and 1% while changes with temperature in the order of a few parts in 10^4 could easily be detected. The experimental error in the absolute value of $\Delta L/L$ amounts to 5% and that in the coefficient of thermal expansion (α) amounts to about 10%. Changes in $\Delta L/L$ of the order of 3×10^{-6} could be detected easily. Measurements were performed at temperature intervals of about 2 K on all samples in the temperature range 77–500 K and in some cases down to 4 K. Four sets of data points were measured for each sample in the case of the velocity of sound and two sets in the case of the thermal expansion measurements. As was done previously [14], smooth curves (figures 1 to 6) were drawn through all the data points (up to about 1000 points, in the case of the velocity of sound for some samples). The scattering in the data points around these smooth curves is less than 0.15% for the velocity of sound and less than 0.5% for $\Delta L/L$.

3. Results

3.1. $c \leqslant 2$ at.% Fe (ISDW phase)

The longitudinal ultrasonic wave velocity for $c < 2$ at.% Fe shows an inverted

λ-type anomaly near the Néel temperature (T_N). Figure 1(a) shows an example of c_L as a function of temperature of 1.5 at.% Fe. On the other hand, the shear wave velocity in these alloys, as well as for $c = 2$ at.% Fe, shows no anomaly at T_N. A representative example is shown for 2 at.% Fe in figure 1(b). The behaviour of the other samples with $c \leqslant 2$ at.% Fe is similar to that shown in figure 1(b). For $c = 2$ at.% Fe, very large ultrasonic attenuation was observed in a small temperature range of about 15 K near the minimum in the v_L versus T curve, making measurements near the minimum point impossible. This large attenuation effect is absent for $c < 2$ at.% Fe. The coefficient of thermal expansion also shows an inverted λ-type behaviour for $c \leqslant 2$ at.% Fe, reaching negative values that become large for $c = 2$ at.% Fe at the minimum point. An example of the α versus T curves is shown in figure 2(a) for $c = 1.5$ at.% Fe and in figure 2(b) for $c = 2.0$ at.% Fe. For $c \leqslant 2$ at.% Fe, $\Delta L/L$ varies continuously through T_N with $|d(\Delta L/L)/dT|$ at T_N increasing as c is increased towards 2 at.% Fe.

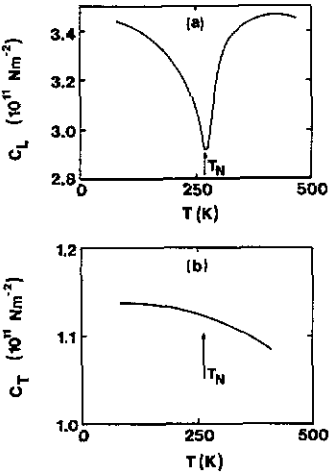

Figure 1. (a) $c_L = \rho v_L^2$, where ρ is the density and v_L is the longitudinal sound velocity, as a function of temperature for Cr + 1.5 at.% Fe. (b) $c_T = \rho v_T^2$, where ρ is the density and v_T is the shear wave velocity, as a function of temperature for Cr + 2 at.% Fe.

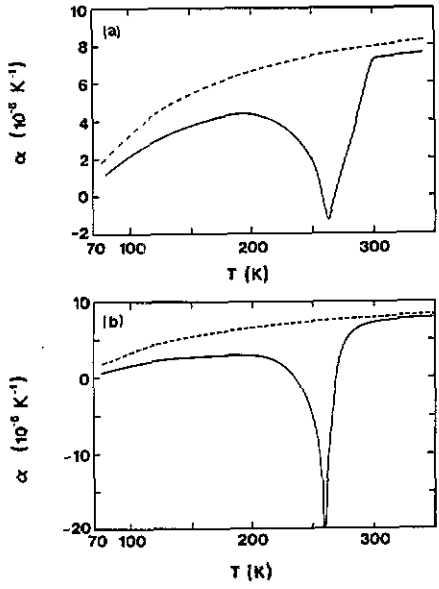

Figure 2. The coefficient of thermal expansion (α) as a function of temperature of (a) Cr + 1.5 at.% Fe and (b) Cr + 2 at.% Fe. The broken line represents α for Cr + 5 at.% V, which remains paramagnetic at all temperatures and which is taken to represent the non-magnetic component of α of the Cr–Fe alloys.

3.2. 2< c <16 at.% Fe (CSDW and RSG phases)

Similarly to $c = 2$ at.% Fe, v_L shows large attenuation near T_N for $c = 2.5$, 4 and 5 at.% Fe. An example is shown in figure 3(a) for 5 at.% Fe. For $5 < c < 16$ at.% Fe v_L could be measured at all temperatures, including those near T_N. The width of the transition becomes smaller as c is increased above 0.5 at.% Fe, reaching its narrowest value around 5 at.% Fe. On increasing c further, the width increases again

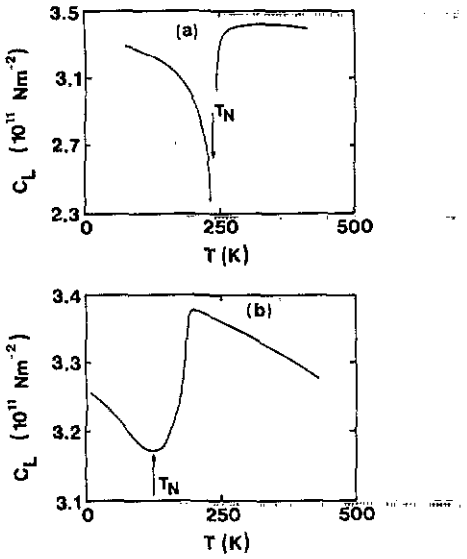

Figure 3. (a) $c_L = \rho v_L^2$, where ρ is the density and v_L is the longitudinal sound velocity, as a function of temperature for Cr + 5 at.% Fe. Due to very large ultrasonic attenuation near T_N, measurements could not be made in a small temperature range around T_N. (b) c_L as a function of temperature for Cr + 12 at.% Fe.

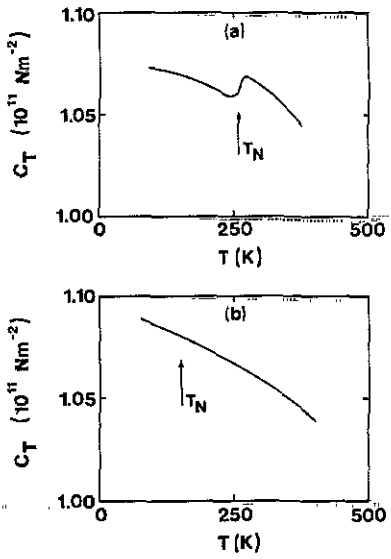

Figure 4. (a) $c_T = \rho v_T^2$, where ρ is the density and v_T is the shear wave velocity, as a function of temperature for Cr + 2.3 at.% Fe. (b) c_T as a function of temperature for Cr + 10 at.% Fe.

as shown for 12 at.% Fe in figure 3(b). The nature of the transition also changes with increasing c. For the lowest concentrations it is of an inverted λ-type, while it becomes more 'jump-like' at higher concentrations (compare figures 3(a) and 3(b)). The behaviour of the shear wave velocity for $c > 2$ at.% Fe differs from that for $c \leqslant 2$ at.% Fe. In the concentration range where v_L shows large attenuation near T_N, a small step in the transverse velocity was observed at T_N as shown in figure 4(a) for $c = 2.3$ at.% Fe. Above 5 at.% Fe this anomaly is again absent (figure 4(b) for 10 at.% Fe), as for $c \leqslant 2$ at.% Fe.

$|\mathrm{d}(\Delta L/L)/\mathrm{d}T|$ of the $\Delta L/L$ versus T curves for $c > 2$ at.% Fe becomes very large near T_N, showing a discontinuity at T_N as shown in figure 5(a) for 4 at.% Fe. Above 4 at.% Fe the $\Delta L/L$ versus T curves again vary smoothly through T_N, as shown in figure 5(b) for $c = 10$ at.% Fe. α for $c = 4$ and 10 at.% Fe is shown in figures 5(c) and 5(d), respectively. No anomalies were observed in either α or v_L that could be identified with ISDW–CSDW transitions.

3.3. 16⩽ c ⩽20 at.% Fe (SG phase)

In this concentration range the temperature variation of the thermal expansion of the Cr–Fe alloys closely follows that of Cr + 5 at.% V, showing no anomalies that could be associated with magnetic or SG transitions. The longitudinal sound velocity and therefore also c_L, however, behave anomalously in the temperature range from 4 to 150 K. This is shown in figures 6(a)–(d) for $c = 16$, 17, 18 and 20 at.% Fe.

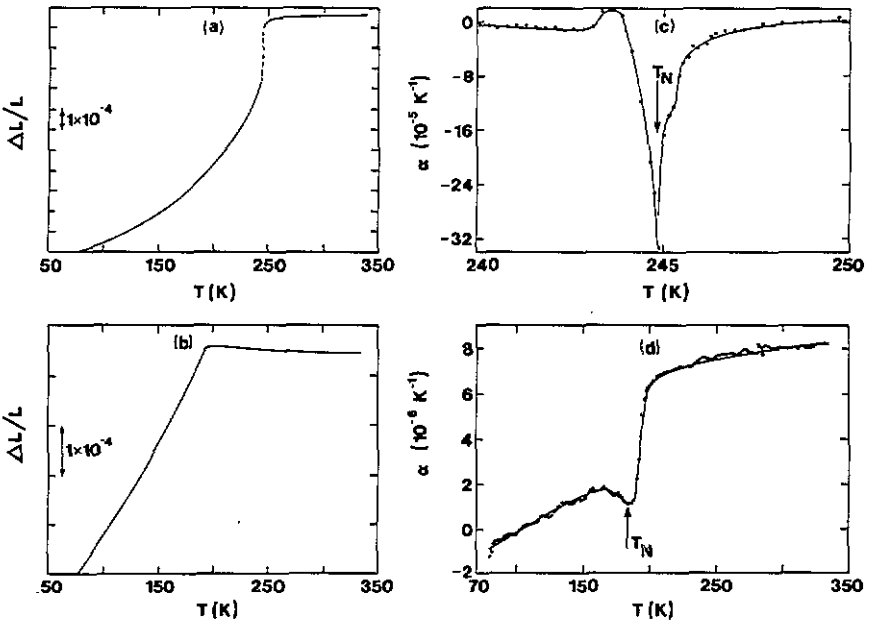

Figure 5. (a) $\Delta L/L$ as a function of temperature for Cr + 4 at.% Fe relative to that for Cr + 5 at.% V. (b) $\Delta L/L$ as a function of temperature for Cr + 10 at.% Fe relative to that for Cr + 5 at.% V. (c) α as a function of temperature for Cr + 4 at.% Fe. (d) α as a function of temperature for Cr + 10 at.% Fe.

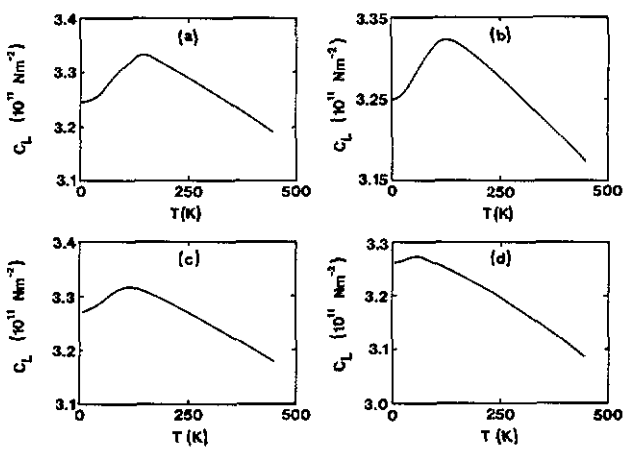

Figure 6. $c_L = \rho v_L^2$, where ρ is the density and v_L is the longitudinal sound velocity, as a function of temperature for (a) Cr + 16 at.% Fe, (b) Cr + 17 at.% Fe, (c) Cr + 18 at.% Fe and (d) Cr + 20 at.% Fe.

3.4. c >20 at.% Fe (ferromagnetic and RSG phases)

No thermal expansion anomalies were observed for $c = 25$ and 30 at.% Fe from 77 K to 450 K. The thermal expansion for these alloys closely follows that of Cr + 5 at.% V. The longitudinal and shear wave velocities also behave normally through the Curie temperatures (T_c).

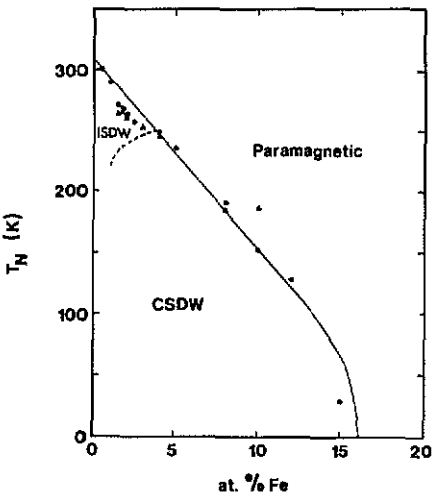

Figure 7. Néel temperatures as a function of Fe concentration for Cr–Fe alloys. The points ● were obtained from the minima in the c_L versus T curves and the points ▲ from the minima in the α versus T curves. The solid and broken lines were constructed from figure 6 of Burke *et al* [9]. They represent average curves through the experimental points of other authors who determined the transition temperatures by techniques other than v_L and α measurements.

4. Discussion

The Néel temperatures of the alloys in the range $0 < c < 16$ at.% Fe are shown in figure 7. T_N is assumed to occur at the minimum points in the c_L versus T and α versus T curves. The solid and broken lines in figure 7 are constructed from figure 6 of Burke *et al* [9]. These lines represent average curves through the experimental points of several authors who determined T_N and T_{IC} by techniques other than v_L and α measurements. Our results for T_N compare well with those determined by the other authors, except for $c = 10$ % for the α measurements, giving credibility to the assumption that T_N occurs at the minima in the α versus T and v_L versus T curves. The minimum in the α versus T curve for $c = 10$ at.% Fe is very shallow compared to that for $c < 10$ at.% Fe, as shown in figures 5(c) and 5(d).

The very large ultrasonic attenuation observed near T_N for $c = 2$, 2.5, 4 and 5 at.% Fe, which is also accompanied by near discontinuities in the $\Delta L/L$ versus T curves, was previously also observed [14] in Cr–Si alloys that show first-order CSDW-P transitions at T_N. In the case of the Cr–Fe alloys we also ascribed these effects to the first order CSDW-P transitions that occur in this system [12].

The structure observed in the α versus T curve for $c = 4$ at.% Fe (figure 5(c)) was also observed [15] in Cr–Si alloys that show first-order CSDW-P transitions. The explanation of this structure is presumably associated with small sample inhomogeneities [15].

The temperature dependence of the elastic constants and the thermal expansion of Cr and its alloys were analysed by Fawcett [16] using a thermodynamic model. In this model the magnetic free energy is given by

$$\Delta F(t,\omega) = \phi(\omega) f(t(\omega)) \tag{1}$$

where $\phi(\omega)$ depends on the volume strain ω, and $t = T/T_0(\omega)$, where $T_0(\omega)$ is a critical temperature parameter. Near the Néel temperature, for $T \rightarrow T_N$ from below or from above, ϕ is assumed to be constant and independent of ω [16]. In the low-temperature region ϕ depends on ω. Taking $f(t) = (1 - t^2)^2$ in this regime, as

was done by Steinemann [17], and assuming $T_0(\omega)$ to be a linear function of ω [16] one obtains for the magnetic contributions to ω and B:

$$\Delta\omega = -(1/B)\,\mathrm{d}(\Delta F)/\mathrm{d}\omega = a_0 + a_1 t^2 + a_2 t^4 \tag{2}$$

where

$$\begin{aligned} a_0 &= -\phi'/B \\ a_1 &= \tfrac{1}{B}(2\phi' - 4\phi\,\mathrm{d}\ln T_0/\mathrm{d}\omega) \\ a_2 &= \tfrac{1}{B}(-\phi' + 4\phi\,\mathrm{d}\ln T_0/\mathrm{d}\omega) \end{aligned} \tag{3}$$

and

$$\Delta B = \mathrm{d}^2(\Delta F)/\mathrm{d}\omega^2 = b_0 + b_1 t^2 + b_2 t^4 \tag{4}$$

where

$$\begin{aligned} b_0 &= \phi'' \\ b_1 &= -2\phi'' + 8\phi'\,\mathrm{d}\ln T_0/\mathrm{d}\omega - 12\phi(\mathrm{d}\ln T_0/\mathrm{d}\omega)^2 \\ b_2 &= \phi'' - 8\phi'\,\mathrm{d}\ln T_0/\mathrm{d}\omega + 20\phi(\mathrm{d}\ln T_0/\mathrm{d}\omega)^2. \end{aligned} \tag{5}$$

$\phi' = \mathrm{d}\phi/\mathrm{d}\omega$ and $\phi'' = \mathrm{d}^2\phi/\mathrm{d}\omega^2$. It is clear that the zero-temperature contributions to $\Delta\omega$ and ΔB come from ϕ' and ϕ'', respectively.

From the above equations it follows that

$$\frac{a_1}{a_0} + \frac{a_2}{a_0} = -1 \tag{6}$$

$$\begin{aligned} \mathrm{d}\ln\phi/\mathrm{d}\omega = \phi'/\phi &= -4\left(\frac{a_1}{a_0} + 2\frac{a_2}{a_0}\right)^{-1}(\mathrm{d}\ln T_0/\mathrm{d}\omega) \\ &= -\frac{8}{\Gamma_0}\left(\frac{\mathrm{d}\ln T_0}{\mathrm{d}\omega}\right)^2\left(\frac{b_1}{b_0} + \frac{b_2}{b_0} + 1\right)^{-1} \end{aligned} \tag{7}$$

$$\mathrm{d}\ln T_0/\mathrm{d}\omega = -\frac{\Gamma_0}{16}\left(5\frac{b_1}{b_0} + 3\frac{b_2}{b_0} + 7\right) \tag{8}$$

where $\Gamma_0 = -\phi''/\phi'$.

$\mathrm{d}\ln\phi/\mathrm{d}\omega$ and $\mathrm{d}\ln T_0/\mathrm{d}\omega$ can be determined from these equations if Γ_0 is known. From (3) and (5) it follows that $\Gamma_0 = b_0/Ba_0$.

Depending on the sign and magnitudes of ϕ, ϕ', ϕ'' and $\mathrm{d}\ln T_0/\mathrm{d}\omega$, the coefficients (a_0, a_1, a_2) and (b_0, b_1, b_2) can be such that $\Delta\omega$ and ΔB can either decrease or increase continuously with increasing temperatures, or first decrease and then increase or vice versa.

In the temperature regions $T \to T_N$ from above or below, Fawcett [16] considered ϕ to be a constant and obtained for these temperature regions the following Grüneisen parameters:

$$\Gamma_{AF} = -\mathrm{d}\ln T_N/\mathrm{d}\omega = -(1/T_N B)\lim_{t\to 1}(\Delta B/\Delta\beta) \qquad t < 1 \tag{9}$$

$$\Gamma_P = -\mathrm{d}\ln T_{sf}/\mathrm{d}\omega = -(1/T_N^{sf} B)\lim_{t\to 1}(\Delta B/\Delta\beta) \qquad t > 1. \tag{10}$$

The subscripts AF and P refer to the antiferromagnetic ($t < 1$) and paramagnetic ($t > 1$) states, respectively, $\Delta\beta = 3\Delta\alpha$ and T_N^{sf} is a spin-fluctuation temperature.

The requirement, that Γ_{AF} and Γ_P in (9) and (10) be determined only in the limit $T \rightarrow T_N$ from above and below, is not stringent [18]. In practice plots of $\Delta B(t)$ versus $\Delta\beta(t)$ both above and below T_N were found to be linear in a relatively wide temperature range near T_N for Cr, and Cr–Mo and Cr–Al alloys [16, 18]. Γ_{AF} and Γ_P can then be determined from these linear parts. However the $\Delta B(t)$ versus $\Delta\beta(t)$ curves for 1.5, 1.8, 2.0 and 2.5 at.% Fe revealed no useful linear parts near T_N in these curves. An example is shown in figure 8 for $c = 1.5$ at.% Fe. We therefore could not determine Γ_{AF} and Γ_P for the Cr–Fe alloys.

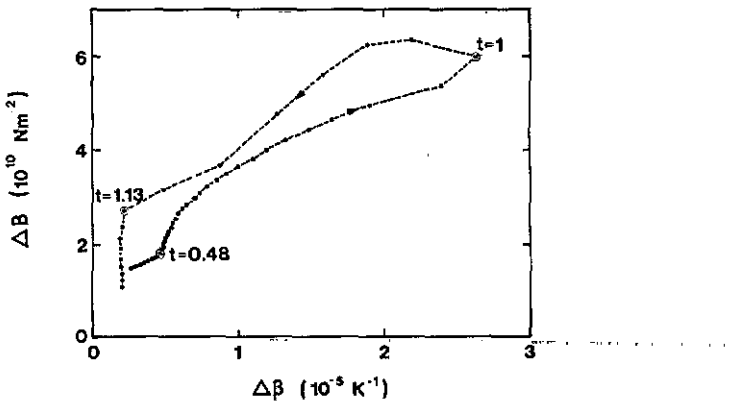

Figure 8. $\Delta B(t)$ as a function of $\Delta\beta(t) = 3\Delta\alpha(t)$ for Cr + 1.5 at.% Fe. The points in the figure were taken at 5 K intervals. $t = T/T_N$.

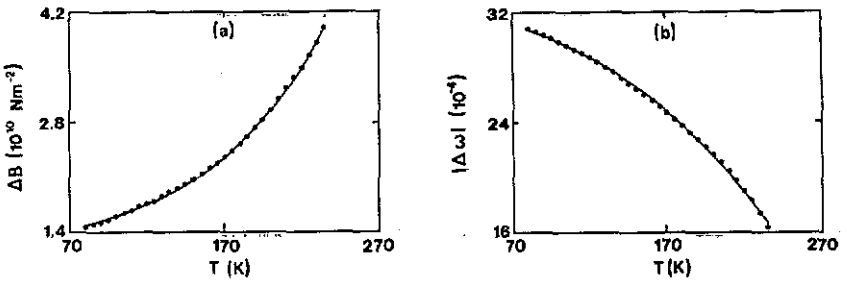

Figure 9. (a) The magnetic contribution to the bulk modulus (ΔB) as a function of temperature for Cr + 1.5 at.% Fe. The solid line is the best fit of the equation $\Delta B = B_0 + B_1T^2 + B_2T^4$. (b) The magnetovolume ($\Delta\omega$) as a function of temperature for Cr + 2 at.% Fe. The solid line is the best fit of the equation $\Delta\omega = A_0 + A_1T^2 + A_2T^4$.

The equations $\Delta\omega(T) = A_0 + A_1T^2 + A_2T^4$ and $\Delta B(T) = B_0 + B_1T^2 + B_2T^4$ were fitted to the experimental results using a least-squares fitting technique. The fits were very good in a temperature range from the lowest temperatures to fairly close to T_N, as shown by two representative examples in figures 9(a) and (b) of $\Delta B(T)$ for 1.5 at.% Fe and $\Delta\omega(T)$ for 2 at.% Fe. As the fits are good to temperatures fairly close to T_N, coefficients (a_0, a_1, a_2) and (b_0, b_1, b_2) in (2) and (4) were calculated from (A_0, A_1, A_2) and (B_0, B_1, B_2) by approximating T_0 with T_N, since the exact value of T_0 is not known. The results are shown in table 1.

Table 1. Néel temperatures (T_N), magnetic contributions to the volume ($\Delta\omega(0)$) and bulk modulus ($\Delta B(0)$) at 0 K, coefficients in the expansions $\Delta\omega(t) = a_0 + a_1t^2 + a_2t^4$ and $\Delta B(t) = b_0 + b_1t^2 + b_2t^4$, $\mathrm{d}\ln T_0/\mathrm{d}\omega$ and $\mathrm{d}\ln\phi/\mathrm{d}\omega$ of Cr–Fe alloys. The experimental errors in $\Delta\omega(0)$ and $\Delta B(0)$ are 10% and 5%, respectively. The standard deviations in obtaining the coefficients (a_0, a_1, a_2) and (b_0, b_1, b_2) vary between 0.2% and 4% for a_0 and b_0, between 3% and 7% for a_1 and b_1 and between 3% and 16% for a_2 and b_2. The values of $\mathrm{d}\ln\phi/\mathrm{d}\omega$ shown in brackets are determined using the values of (a_0, a_1, a_2) in equation (7) and those not in brackets from the values of (b_0, b_1, b_2). * Values determined from the minima in v_L are given.

					$\Delta\omega = a_0 + a_1t^2 + a_2t^4$			$\Delta B = b_0 + b_1t^2 + b_2t^4$				
at.% Fe	$T_N(K)^*$	$\Delta\omega(0)(\times10^{-4})$	$\Delta B(0)(\times10^9 Nm^{-2})$	$\Gamma_0 = \frac{1}{B}\frac{\Delta B(0)}{\Delta\omega(0)}$	$a_0(\times10^{-3})$	$a_1(\times10^{-3})$	$a_2(\times10^{-3})$	$b_0(\times10^9 Nm^{-2})$	$b_1(\times10^9 Nm^{-2})$	$b_2(\times10^9 Nm^{-2})$	$d\ln T_0/d\omega$	$d\ln\phi/d\omega$
0.5	300	–	4.5	–	–	–	–	5.21	23.31	−0.77	–	–
1.0	289	–	9.3	–	–	–	–	9.95	12.36	24.05	–	–
1.5	270	−21.0	12.3	−29.4	−2.05	0.985	0.320	13.37	15.84	25.03	34.1	(171.8) 77.8
1.8	267	−18.5	15.4	−41.4	−1.83	1.044	0.120	16.04	22.88	18.50	45.6	(260.1) 112.3
2.0	262	−32.0	16.6	−26.1	−3.22	1.610	0.368	17.03	21.28	23.33	28.3	(155.5) 70.9
2.5	256	−39.5	18.5	−23.4	−4.02	2.003	0.376	20.42	20.71	23.28	22.7	(132.5) 55.7
4.0	248	−36.2	18.9	−26.1	−3.63	1.491	1.125	20.72	26.13	15.97	25.5	(99.0) 65.6
5.0	235	–	16.0	–	–	–	–	18.27	12.66	42.59	–	–
8.0	190	−20.8	16.9	−40.8	−2.10	1.568	0.071	20.3	18.5	26.7	39.6	(194.5) 95.7
10.0	152	−14.5	16.0	−51.6	−1.64	2.045	−0.440	16.66	31.45	−8.41	48.1	(270.9) 150.7
12.0	128	–	15.0	–	–	–	–	15.68	17.35	−10.18	–	–
15.0	90	–	11.8	–	–	–	–	12.50	−2.47	−1.16	–	–

We tested equation (6) for $c = 1.5$, 1.8, 2, 2.5, 4, 8 and 10 at.% Fe and obtained $(a_1/a_0 + a_2/a_0) = -0.637$, -0.637, -0.613, -0.587, -0.720, -0.782 and -0.977, respectively. These values are in reasonable agreement with the value of -1 if the approximations in the thermodynamic theory are kept in mind.

Table 1 also shows values of $\mathrm{d}\ln T_0/\mathrm{d}\omega$ and $\mathrm{d}\ln\phi/\mathrm{d}\omega$ calculated using (7) and (8) and Γ_0 (given in this table). Shown in the table are values of $\mathrm{d}\ln\phi/\mathrm{d}\omega$ calculated from (7) using values of (a_0, a_1, a_2) and (b_0, b_1, b_2), respectively. The values of $\mathrm{d}\ln\phi/\mathrm{d}\omega$ using (a_0, a_1, a_2) are about twice as large as those using (b_0, b_1, b_2). The reason for the discrepancy is unknown but may partly be attributed to the approximations made in the thermodynamic model. The values of $\mathrm{d}\ln T_0/\mathrm{d}\omega$ and $\mathrm{d}\ln\phi/\mathrm{d}\omega$ are of the same order of magnitude as those determined for pure Cr by Fawcett [16] (25 and 70, respectively) using specific heat and magnetoelastic data. Our values for Cr–Fe were determined solely from the magnetoelastic data. We conclude that the thermodynamic model, with $f(t) = (1 - t^2)^2$ and T_0 approximated by T_N, describes the temperature behaviour of $\Delta B(T)$ and $\Delta\omega(T)$ for SDW Cr–Fe alloys reasonably well. From table 1, $\Delta B(0)$ tends to reach a maximum value between 2.5 and 4 at.% Fe, while $\Delta\omega(0)$ tends towards a minimum value in this concentration range. Also from the table, one notes that both $\mathrm{d}\ln T_0/\mathrm{d}\omega$ and $\mathrm{d}\ln\phi/\mathrm{d}\omega$ roughly tend to minimum values at 2.5 at.% Fe, which is close to the triple point on the magnetic phase diagram.

Although we studied several alloys close to the triple point with $c = 1.5$, 1.8, 2.0 and 2.5 at.% Fe, we failed to observe any effect that can be ascribed to CSDW–ISDW phase transitions at T_{IC}. Also we did not observe this transition in v_L of an alloy with $c = 2.3$ at.% Fe. Usually, very well defined anomalies are observed in the coefficient of thermal expansion at CSDW–ISDW transitions of Cr alloys [14, 19]. Its absence for our Cr–Fe alloys is probably due to T_{IC} being too close to T_N to be resolved. Butylanko [20], however, observed two anomalies in $\Delta L/L$ versus T curves for Cr–Fe alloys close to the triple point. One of these anomalies is in the form of a sharp jump in $\Delta L/L$ at T_{IC} and the other is a faint anomaly at T_N. In all our alloys near the triple point we observed only a jump-like anomaly without any evidence of a faint anomaly appearing at a higher temperature. We identified the jump in $\Delta L/L$ with T_N, which is supported by the v_L measurements.

The re-entrant spin-glass transition was not observed in the velocity of sound measurements for $c = 12$ and 15 at.% Fe. Below T_N, c_L varies smoothly down to 4 K in the antiferromagnetic alloys with $c < 16$ at.% Fe without any trace of an anomaly at the RSG transition. Within the sensitivity of our measurements no anomalies were observed in c_L or $\Delta L/L$ in the ferromagnetic alloys at their Curie temperatures. It may be mentioned that the thermal expansion measurements of Acet *et al* [21] on ferromagnetic $Cr_{75}Fe_{21.3}Mn_{3.7}$ did not reveal any anomaly at T_c or at the RSG transition temperature. Measurements using neutron scattering techniques [9], do, however, indicate that Cr–Fe alloys are ferromagnetic above 19 at.% Fe. The absence of anomalies in v_L and $\Delta L/L$ near T_c for ferromagnetic Cr–Fe alloys in the range $20 \leqslant c \leqslant 30$ at.% Fe may be connected with long-range inhomogeneities in the magnetization distribution, as suggested by Burke *et al* [9].

The alloys containing 16, 17, 18 and 20 at.% Fe which are, according to the magnetic phase diagram of Burke *et al* [9], in the SG or RSG phase at low temperatures show no anomalies in the $\Delta L/L$ versus T curves at temperatures above 77 K. Due to technical problems in using strain gauges down to 4 K, we did not perform $\Delta L/L$ measurements down to helium temperatures. For the above-mentioned alloys, $\alpha(T)$

closely follows that for paramagnetic Cr + 5 at.% V at all temperatures between 77 and 450 K. On the other hand, these alloys do show anomalies in v_L, and thus also in c_L, below about 150 K, as depicted in figures 6(a), (b), (c) and (d). The anomalies appear as a softening of the mode below 150 K with a small peak in the c_L versus T curves between 4 K and 150 K (figure 6). The anomalies are roughly of the type predicted for the SG transition [3–6], and start at temperatures well above the spin-glass transition temperatures for these alloys $T_g \approx 30$ K [9]. As the SG region is very narrow (between 16 and 19 at.% Fe, with the antiferromagnetic phase below 16 at.% Fe and the ferromagnetic phase above 19 at.% Fe) we are of the opinion that the anomalies seen in the alloys containing 16, 17, 18 and 20 at.% Fe are combined effects of the SG transition and some SDW transition still left in these samples. Support for this comes from the work of Loegel [22] who suggests contrary to the later work [9], that the antiferromagnetic and ferromagnetic regions overlap between 16 and 20 at.% Fe. We thus did not attempt to test the prediction [8] that the sound speed for SG alloys should vary as $(T - T_g)$.

5. Conclusions

We have studied the velocity of sound and thermal expansion of Cr–Fe alloys in all possible magnetic phases of this system in detail. Well defined anomalies were observed in the longitudinal velocity of sound and the thermal expansion at the Néel temperatures of the antiferromagnetic alloys. No anomalies were observed in the transverse sound velocity of the antiferromagnetic alloys which show second-order ISDW–P transitions at T_N. A small step was, however, observed in the shear-wave velocity at T_N in alloys showing a first order CSDW–P transition. The temperature dependence of the magnetic components of the bulk modulus and the thermal expansion is fairly well described by the thermodynamic model.

Within experimental error, no anomalies were observed in either the velocity of sound or the thermal expansion at the Curie temperatures of the ferromagnetic alloys. Anomalies were observed in the velocity of sound in the SG Cr–Fe alloys between 4 and 150 K. However, these anomalies can not be attributed solely to the SG transition since some antiferromagnetic component may still be left in them. No anomalies in either the sound velocity or the thermal expansion were observed that could be identified with CSDW–ISDW phase transitions.

Acknowledgments

Financial aid from the Foundation for Science and Development is acknowledged, as well as technical assistance from T Germishuyse.

References

[1] Mukhopadhyay P K and Raychandhuri A K 1990 *J. Appl. Phys.* **67** 5235
[2] Mukhopadhyay P K and Raychandhuri A K 1988 *J. Phys. C: Solid State Phys.* **21** L385
[3] Hawkins G F and Thomas R L 1978 *J. Appl. Phys.* **49** 1627
[4] Hawkins G F, Thomas R L and de Graaf A M 1979 *J. Appl. Phys.* **50** 1709
[5] Huang F S 1983 *J. Appl. Phys.* **54** 5718

[6] Doussineau P, Levelut A, Matecki M, Renard J P and Schön W 1987 *Europhys. Lett.* **3** 251
[7] Hawkins G F, Moran T J and Thomas R L 1977 *Amorphous Magnetism II* ed R A Lavy and R Hasegawa (New York: Plenum) p 117
[8] Hertz J A, Khurana A and Klemm R A 1981 *Phys. Rev. Lett.* **46** 496
[9] Burke S K, Cywinski R, Davis J R and Rainford B D 1983 *J. Phys. F: Met. Phys.* **13** 451
[10] Böni P and Shapiro S M 1989 *J. Phys.: Condens. Matter* **1** 6123
[11] Hausch G and Török E 1977 *Phys. Status Solidi* a **40** 55
[12] Suzuki T 1976 *J. Phys. Soc. Japan* **41** 1187
[13] Alberts H L and Lourens J A J 1984 *Phys. Rev.* B **29** 5279
[14] Alberts H L and Lourens J A J 1988 *J. Phys. F: Met. Phys.* **18** 123
[15] Lourens J A J and Wostenholm G H 1991 *J. Magn. Magn. Mater.* **96** 301
[16] Fawcett E 1989 *J. Phys.: Condens. Matter* **1** 203
[17] Steinemann S G 1978 *J. Magn. Magn. Mater.* **7** 84
[18] Fawcett E and Alberts H L 1990 *J. Phys.: Condens. Matter* **2** 6251
[19] Alberts H L and Lourens J A J 1988 *J. Phys. F: Met. Phys.* **18** L213
[20] Butylenko A K 1989 *Phys. Met. Metall.* **68** 37
[21] Acet M, Schneider T, Zähres H, Stamm W, Wassermann E F and Pepperhoff W 1989 *Physica* B **161** 63
[22] Loegel B 1975 *J. Phys. F: Met. Phys.* **5** 497